



UNIVERSITI PUTRA MALAYSIA

**DIELECTRIC PROPERTIES OF ND-DOPED YTTRIUM IRON GARNET
AND CU OR CO-DOPED NICKEL ZINC FERRITES**

KHE CHENG SEONG.

FS 2006 13

**DIELECTRIC PROPERTIES OF Nd-DOPED YTTRIUM IRON GARNET
AND Cu OR Co-DOPED NICKEL ZINC FERRITES**

By

KHE CHENG SEONG

**Thesis Submitted to the School of Graduate Studies, Universiti Putra Malaysia,
in Fulfilment of the Requirements for the Degree of Master of Science**

January 2006



DEDICATION

I would like to dedicate this thesis to family members and all my friends.



Abstract of thesis presented to Senate of Universiti Putra Malaysia in fulfilment of the requirements for the degree of Master of Science

**DIELECTRIC PROPERTIES OF Nd-DOPED YTTRIUM IRON GARNET
AND Cu OR Co-DOPED NICKEL ZINC FERRITES**

By

KHE CHENG SEONG

January 2006

Chairman :Jumiah Binti Hassan, PhD

Faculty :Science

In this work, three series of soft ferrites were synthesized via solid state route. These are $\text{Ni}_{0.3-x}\text{Cu}_x\text{Zn}_{0.7}\text{Fe}_2\text{O}_4$ ($x= 0.0, 0.05, 0.10, 0.15, 0.20, 0.25$ and 0.30), $\text{Ni}_{0.5-x}\text{Co}_x\text{Zn}_{0.5}\text{Fe}_2\text{O}_4$ ($x=0.0, 0.1, 0.2, 0.3, 0.4,$ and 0.5) and $\text{Y}_{3-x}\text{Nd}_x\text{Fe}_5\text{O}_{12}$ ($x=0.0, 0.4, 0.8, 1.2$ and 1.6). The X-ray diffraction patterns showing single phases for these three samples series, confirmed that the spinel and garnet structure had been formed in the Ni-Zn ferrites and YIG respectively.

Ni-Zn ferrites substituted with copper oxide showed exaggerated grain growth whereas the other series substituted with cobalt oxide had no massive changes in the microstructure. For the YIG substituted with neodymium oxide, the first sample exhibited a porous microstructure and developed to become a more compact and poreless microstructure as neodymium increased.

Measurement of the electrical properties was carried out in the temperature range from 28°C to 300°C in the low frequency region of 10 Hz to 1 MHz. Impedance



analyzer was employed in the ac data acquisition whereas a pico-ammeter and a dc voltage source were used to measure electric current at different voltages.

The results obtained from dielectric measurements indicate that microstructure of the samples plays an important role in the dielectric dispersion. A sample with higher porosity is associated with a low value of dielectric permittivity due to its high resistivity. Meanwhile a sample with a more compact structure exhibits higher dielectric permittivity due to its higher conductivity. Hence, electron hopping between Fe^{2+} and Fe^{3+} would increase in the conductive sample and give higher dielectric permittivity if compared with the resistive one.

The dielectric response for every sample in the three series of soft ferrites displayed different mechanisms throughout the investigated temperature range. Therefore, dielectric behaviour of a sample can be modeled into at least two equivalent circuits.

The complex impedance plots of both samples Ni-Zn ferrites and YIG showed overlapping semicircles. However, at high temperature the high frequency arc disappeared and there remained just one semicircle. The center of the semicircle for all samples was depressed below the real impedance axis and described by the parameter α . The results indicate that all these three series of soft ferrites can be represented by two parallel RC circuits connected in series that correspond to the contributions of grain and grain boundary.

The ac conductivity for the three series of soft ferrites showed almost similar behaviour. At lower temperature, the ac curves can be divided into two region. The

low frequency region showed that the ac conductivity was weakly dependent on frequency whereas at high frequency region, it was strongly dependent on frequency. As the temperature increased, the ac conductivity seemed independent of frequency. Extrinsic and intrinsic conductions had been inferred to occur in these samples.

It is also found that microstructural entities such as grains and porosity play an important role in the dc resistivity. The two activation energies obtained indicated that there were probably two parallel conduction mechanisms or spin reorientation phase transition occurred.

Abstrak tesis yang dikemukakan kepada Senat Universiti Putra Malaysia sebagai memenuhi keperluan untuk ijazah Master Sains

**SIFAT DIELEKTRIK GARNET BESI YTTRIUM YANG DIDOPKAN
DENGAN Nd DAN FERIT NIKEL ZINK YANG DIDOPKAN DENGAN
Cu ATAU Co**

Oleh

KHE CHENG SEONG

January 2006

Pengerusi :Jumiah binti Hassan, PhD

Fakulti :Sains

Dalam kajian ini, tiga siri ferit lembut telah disediakan melalui tindak balas keadaan pepejal. Ferit yang dimaksudkan adalah $Ni_{0.3-x}Cu_xZn_{0.7}Fe_2O_4$ ($x= 0.0, 0.05, 0.10, 0.15, 0.20, 0.25$ and 0.30), $Ni_{0.5-x}Co_xZn_{0.5}Fe_2O_4$ ($x=0.0, 0.1, 0.2, 0.3, 0.4,$ and 0.5) dan $Y_{3-x}Nd_xFe_5O_{12}$ ($x=0.0, 0.4, 0.8, 1.2$ and 1.6). Pembelauan sinar-x mengesahkan kesemua sampel dalam fasa tunggal dengan struktur spinel dan garnet.

$Ni_{0.3-x}Cu_xZn_{0.7}Fe_2O_4$ didapati mengalami proses pertumbuhan butiran yang ketara manakala $Ni_{0.5-x}Co_xZn_{0.5}Fe_2O_4$ tiada perubahan yang ketara dalam mikrostruktur. Untuk $Y_{3-x}Nd_xFe_5O_{12}$, pada mulanya menunjukkan liang yang banyak tetapi kemudian menjadi semakin tumpat dan kurang liang apabila kandungan neodymium meningkat.

Pengukuran sifat elektrik telah dilakukan pada julat suhu diantara $28^{\circ}C$ dan $300^{\circ}C$ pada frekuensi rendah daripada 10 Hz hingga 1 MHz. Mesin analisis impedans telah digunakan untuk memperolehi data ac manakala piko ammeter dan punca voltan dc digunakan untuk pengukuran arus terus pada voltan yang berlainan.



Daripada sifat dielektrik yang diperolehi, didapati mikrostruktur memainkan peranan yang penting. Sampel yang mempunyai liang yang banyak mempunyai nilai dielektrik yang rendah. Ini disebabkan sampel yang mempunyai lebih keliangan mempunyai rintangan yang lebih besar dan seterusnya melarang elektron yang melompat di antara Fe^{2+} dan Fe^{3+} yang menyebabkan polarisasi dalam ferit.

Sifat dielektrik untuk setiap sampel dalam tiga siri ferit ini menunjukkan mekanisme yang berlainan pada suhu yang berbeza. Jadi, satu sampel biasanya boleh diwakili oleh sekurang-kurangnya dua model litar setara dalam julat suhu kajian ini.

Komplek impedans untuk ketiga-tiga sampel ferit lembut menunjukkan dua lengkung semibulatan bertindih. Akan tetapi, pada suhu yang tinggi, lengkung semibulatan pada frekuensi yang tinggi lenyap dan meninggalkan hanya satu lengkung semibulatan. Semua semibulatan mempunyai pusat yang tertekan ke bawah paksi nyata impedans. Keputusan menunjukkan kebanyakan sampel boleh diwakili oleh dua litar RC yang selari disambung secara siri yang disebabkan oleh butiran dan sempadan butiran sampel.

Konduktiviti ac untuk ketiga-tiga siri sampel ini menunjukkan kelakuan yang agak sama. Pada suhu yang rendah, lengkung ac boleh dibahagikan kepada dua bahagian. Pada bahagian frekuensi rendah, kekonduksian ac bergantung lemah terhadap frekuensi manakala pada frekuensi tinggi, ia bergantung kuat kepada frekuensi. Apabila suhu meningkat, kekonduksian ac hampir tidak bergantung kepada frekuensi. Kekonduksian ekstrinsik dan intrinsik dipercayai berlaku dalam sampel-sampel ini.

Mikrostruktur seperti butiran dan liang didapati memainkan peranan yang penting dalam kekonduksian arus terus. Dua tenaga pengaktifan diperolehi dipercayai disebabkan oleh kewujudan dua mekanisma kekonduksian yang selari atau fasa translasi putaran reorientasi telah berlaku.

ACKNOWLEDGEMENT

First and foremost, I would like to express my highest gratitude to Dr. Jumiah Hassan, as my project supervisor, Assoc. Prof. Dr. Wan Mohd Daud Wan Yusoff and Assoc. Prof. Dr. Mansor Hashim as my co-supervisors for giving the guidance, suggestions and knowledge in the dielectric theories and also in the ferrite materials.

I would like to thank Mr. Woon, lecturer from UNITEN, my lab-mate, Tay, Walter Charles, INFOPORT staff, XRD lab assistant and many others who had help me through out this project where without their invaluable help this project could not have been completed with success.

I also would like to acknowledge Universiti Putra Malaysia for the financial support under the PASCA scheme.

Finally, I would like to express my fullest appreciation to my family members especially to my parents for their support and understanding from the very beginning of my work until this studies were completed.



I certify that an Examination Committee has met on 25th January 2006 to conduct the final examination of Khe Cheng Seong on his Master of Science thesis entitled “Dielectric Properties of Nd-Doped Yttrium Iron Garnet and Cu- or Co-Doped Nickel Zinc Ferrites” in accordance with Universiti Pertanian Malaysia (Higher Degree) Act 1980 and Universiti Pertanian Malaysia (Higher Degree) Regulations 1981. The Committee recommends that the candidate be awarded the relevant degree. Members of the Examination Committee are as follows:

MOHD. MAAROF H.A MOKSIN, PhD

Professor
Faculty of Science
Universiti Putra Malaysia
(Chairman)

ABDUL HALIM SHAARI, PhD

Professor
Faculty of Science
Universiti Putra Malaysia
(Internal Examiner)

ZAIDAN ABDUL WAHAB, PhD

Associate Professor
Faculty of Science
Universiti Putra Malaysia
(Internal Examiner)

IBRAHIM ABU TALIB, PhD

Professor
Faculty of Science and Technology
Universiti Kebangsaan Malaysia
(External Examiner)



HASANAH MOHD. GHAZALI, PhD

Professor/Deputy Dean
School of Graduate Studies
Universiti Putra Malaysia

Date: **27 MAR 2006**



This thesis submitted to the senate of Universiti Putra Malaysia and has been accepted fulfilment of the requirement for the degree of Master of Science. The members of the Supervisor Committee are as follows:

JUMIAH HASSAN, PhD

Lecturer
Faculty of Science
Universiti Putra Malaysia
(Chairman)

WAN MOHD. DAUD WAN YUSOFF, PhD

Associate Professor
Faculty of Science
Universiti Putra Malaysia
(Member)

MANSOR HASHIM, PhD

Associate Professor
Faculty of Science
Universiti Putra Malaysia
(Member)




AINI IDERIS, PhD
Professor/Dean
School of Graduate Studies
Universiti Putra Malaysia

Date: **13 APR 2006**



DECLARATION

I hereby declare that the thesis is based on my original work except for quotations and citations which have been duly acknowledged. I also declare that it has not been previously or concurrently submitted for any other degree at UPM or other institutions.



KHE CHENG SEONG
Date: 27/2/06

TABLE OF CONTENTS

	Page
DEDICATION	ii
ABSTRACT	iii
ABSTRAK	vi
ACKNOWLEDGEMENT	iv
APPROVAL	v
DECLARATION	xii
LIST OF TABLES	xv
LIST OF FIGURES	xix
LIST OF PLATES	xxv
LIST OF ABBREVIATIONS	xxvi
CHAPTER	
1 INTRODUCTION	
1.1 Introduction	1
1.2 Objectives	2
1.3 Research Overview	3
2 LITERATURE REVIEW	
2.1 Dielectric Properties of Solid	4
2.2 Dielectric Properties of Ferrites	7
2.3 AC Electrical conductivity	8
2.4 DC Electrical conductivity	9
3 THEORY	
3.1 Spinel Structure	12
3.2 Garnet Structure	13
3.3 Dielectric Definition	15
3.4 Dielectric Polarization	15
3.5 Dielectric Models	
3.5.1 Debye Expression	20
3.5.2 Cole-Cole Expression	21
3.5.3 Power Law Relation	22
3.6 Alternating Current Conductivity	25
3.7 Complex Plane Analysis	26
3.8 DC conductivity	30
4 METHODOLOGY	
4.1 Sample Preparation	31
4.2 AC Measurement	38
4.3 DC Measurement	38
4.4 Structure Analysis	39
4.5 Microstructural Analysis	39
4.6 Density	40



5	RESULTS AND DISCUSSION	
5.1	X-Ray Diffraction Patterns	
5.1.1	Nickel Zinc Ferrites Substituted With Copper	41
5.1.2	Nickel Zinc Ferrites Substituted With Cobalt	42
5.1.3	Yttrium Iron Garnet Substituted With Neodymium	43
5.2	Microstructural Analysis	
5.2.1	Nickel Zinc Ferrites Substituted With Copper	44
5.2.2	Nickel Zinc Ferrites Substituted With Cobalt	48
5.2.3	Yttrium Iron Garnet Substituted With Neodymium	50
5.3	Dielectric Properties in Frequency Domain	
5.3.1	Nickel Zinc Ferrites Substituted With Copper	52
5.3.1.1	Negative Capacitance	60
5.3.2	Nickel Zinc Ferrites Substituted With Cobalt	62
5.3.3	Yttrium Iron Garnet Substituted With Neodymium	72
5.4	Dielectric Response with Equivalent Circuit Modeling	
5.4.1	Nickel Zinc Ferrites Substituted With Cobalt	83
5.4.2	Nickel Zinc Ferrites Substituted With Copper	95
5.4.3	Yttrium Iron Garnet Substituted With Neodymium	114
5.5	Complex Impedance Plot	
5.5.1	Nickel Zinc Ferrites Substituted With Copper	127
5.5.2	Nickel Zinc Ferrites Substituted With Cobalt	144
5.5.3	Yttrium Iron Garnet Substituted With Neodymium	157
5.6	AC Conductivity In Frequency Domain	
5.6.1	Nickel Zinc Ferrites Substituted With Copper	172
5.6.2	Nickel Zinc Ferrites Substituted With Cobalt	176
5.6.3	Yttrium Iron Garnet Substituted With Neodymium	179
5.7	DC Resistivity	
5.7.1	Nickel Zinc Ferrites Substituted With Copper	182
5.7.2	Nickel Zinc Ferrites Substituted With Cobalt	186
5.3.3	Yttrium Iron Garnet Substituted With Neodymium	189
6	CONCLUSION AND SUGGESTION	
6.1	Conclusions	192
6.2	Suggestions	194
	REFERENCES	195
	APPENDICES	198
	BIODATA OF THE AUTHOR	200



LIST OF TABLES

Table	Page
3.1 Capacitance values and their possible interpretation.	29
4.1 Starting materials for preparing yttrium iron garnet.	31
4.2 Starting materials for preparing nickel zinc ferrites.	31
4.3 Yttrium iron garnet substituted with neodymium ($Y_{3-x}Nd_xFe_3O_{12}$)	33
4.4 Nickel zinc ferrites substituted with copper ($Ni_{0.3-x}Cu_xZn_{0.7}Fe_2O_4$)	33
4.5 Nickel zinc ferrites substituted with cobalt ($Ni_{0.5-x}Co_xZn_{0.5}Fe_2O_4$)	34
5.1 Density and average grain size of nickel zinc ferrites substituted with copper.	44
5.2 Average grain size and density of nickel zinc ferrites substituted with cobalt.	48
5.3 Density and average grain size of YIG substituted with neodymium.	50
5.4 Activation energies of peak frequency for sample N1 to N7.	56
5.5 Activation energies of loss peak frequency, F_p for different samples.	66
5.6 Activation energy of F_p for samples Y1 to Y5.	76
5.7 Theoretical values for fitting the experimental data for sample CC from (a) 28°C to 150°C (b) 200°C to 300°C.	87
5.8 Theoretical values for fitting the experimental data for sample C1 from (a) 28°C to 100°C (b) 150°C to 300°C.	88
5.9 Theoretical values for fitting the experimental data for sample C3 from (b) 28°C to 200°C (b) 250 and 300°C.	89
5.10 Theoretical values for fitting the experimental data for sample C4 from (a) 28°C to 50°C (b) 100°C to 300°C.	89
5.11 Theoretical values for fitting the experimental data for sample C5 from (a) 28°C to 100°C (b) 150°C to 300°C.	90
5.12 Theoretical values for fitting the experimental data for sample C2 from 28°C to 300°C.	94



5.13	Theoretical values for fitting the experimental data for sample N1 from (a) 28°C to 100°C (b) 150°C to 300°C.	101
5.14	Theoretical value for fitting the experimental data for sample N2 from (a) 28°C to 150°C (b) 200°C to 300°C.	102
5.15	Theoretical values for fitting the experimental data for sample N3 at (a) 28°C (b) 50°C to 300°C.	102
5.16	Theoretical values for fitting the experimental data for sample N6 from (a) 28°C to 100°C (b) 150°C to 300°C.	103
5.17	Theoretical values for fitting the experimental data for sample N7 from (a) 28°C to 150°C (b) 200°C to 300°C.	103
5.18	Theoretical values for fitting the experimental data for sample N4 from (a) 28°C to 100°C (b) 150°C to 200°C (c) 250°C to 300°C.	109
5.19	Theoretical values for fitting the experimental data for sample N5 from (a) 28°C and 100°C (b) 150°C to 250°C.	113
5.20	Theoretical values for fitting the experimental data for sample Y1 from (a) 28°C to 150°C (b) 200°C to 300°C.	118
5.21	Theoretical values for fitting the experimental data for sample Y2 from (a) 28°C to 50°C (b) 100°C to 300°C.	119
5.22	Theoretical values for fitting the experimental data for sample Y3 from (a) 28°C to 200°C (b) 250°C and 300°C.	120
5.23	Theoretical values for fitting the experimental data for sample Y4 from (a) 28°C to 150°C (b) 200°C and 300°C.	120
5.24	Theoretical values for fitting the experimental data for sample Y5 from (a) 28°C to 150°C (b) 200°C to 300°C.	126
5.25	Values of fitted parameters for different samples at room temperature.	133
5.26	Theoretical values for fitting the experimental data of sample N4 at (a) 50°C to 100°C (b) 150°C to 300°C.	135
5.27	Theoretical values for fitting the experimental data of sample N5 at (a) 50°C to 150°C (b) 200°C to 300°C.	136
5.28	Theoretical values for fitting the experimental data of sample N1 at (a) 50°C and (b) 100°C to 300°C.	139



5.29	Theoretical values for fitting the experimental data of sample N2 at (a)50°C and (b)100°C to 300°C.	142
5.30	Theoretical values for fitting the experimental data of sample N3 from 50°C to 300°C.	142
5.31	Theoretical values for fitting the experimental data of sample N6 at (a)50°C to 100°C (b) 150°C to 300°C.	143
5.32	Theoretical values for fitting the experimental data of sample N7 at (a)50°C to 100°C (b) 150°C to 300°C.	143
5.33	Values of capacitance and resistance and the other parameters obtained from fitting for different samples at room temperature.	149
5.34	Theoretical values that used to fit the experimental data of sample C1 at (a) 50°C (b) 100°C to 300°C.	154
5.35	The resistances and the capacitances that obtained from the curve fitting for different samples at various temperatures.	156
5.36	Value of fitted parameters for sample Y2 from (a) 28°C to 100°C (b)150°C to 300°C	161
5.37	Theoretical values for fitting the experimental data for sample Y5 from 28°C to 300°C.	167
5.38	Theoretical values for fitting the experimental data for sample Y1 from (a) 28°C to 100°C (b) 150°C to 300°C	167
5.39	Theoretical values for fitting the experimental data for sample Y3 from (a) 28°C and 50°C (b) 100°C to 300°C.	168
5.40	Theoretical values for fitting the experimental data for sample Y4 from (a) 28°C to 150°C and (b) 200°C to 300°C.	169
5.41	Values of resistance and capacitance for sample Y1 to Y5 at room temperature.	169
5.42	Activation energies of different samples at low and high temperature regions.	175
5.43	Activation energies of different samples at low and high temperature regions.	178

5.44	Activation energies of different samples at low and high temperature regions.	181
5.45	Activation energies of samples N1 to N7.	185
5.46	Activation energy calculated from Figure 5.78.	188
5.47	Activation energy of different samples.	190



LIST OF FIGURES

Figure		Page
3.1	Spinel structure.	13
3.2	Garnet structure.	14
3.3	Various types of polarization.	19
3.4	The probable occurrence of the various types of the polarization and the dependence of the permittivity with respect to frequency.	20
3.5	The frequency dependence of the real and imaginary parts of the permittivity of an Ideal Debye system corresponding to equation.	21
3.6	The frequency dependence of the real and imaginary parts of the permittivity corresponding to the Cole-Cole expression.	22
3.7	The bound dipolar dispersion.	23
3.8	The quasi-dc dispersion.	24
3.9	A schematic representation of the various observed types of dielectric response in the entire range of solids.	25
3.10	Equivalent circuit proposed for sample ferrites.	27
3.11	Sketch of a complex impedance plot showing various parameters.	28
3.12	The current of an ohmic material plotted versus the potential difference across it.	30
4.1	Procedure of sample preparation ($\text{Ni}_{0.3-x}\text{Cu}_x\text{Zn}_{0.7}\text{Fe}_2\text{O}_4$).	35
4.2	Procedure of sample preparation ($\text{Ni}_{0.5-x}\text{Co}_x\text{Zn}_{0.7}\text{Fe}_2\text{O}_4$).	36
4.3	Procedure of sample preparation ($\text{Y}_{3-x}\text{Nd}_x\text{Fe}_5\text{O}_{12}$).	37
5.1	XRD patterns of nickel zinc ferrite substituted with copper.	41
5.2	XRD patterns of nickel zinc ferrites substituted with cobalt.	42
5.3	XRD patterns of yttrium iron garnet substituted with neodymium.	43



5.4	Diagrammatic representation the successive stages in the joining of two of grains by sintering.	44
5.5	Complex dielectric permittivity of samples N1 to N7 at room temperature (a) dielectric permittivity (b) loss factor.	52
5.6	Dielectric properties of sample N2 at different temperature.	55
5.7	Arrhenius plot for sample N2.	56
5.8	Dielectric properties of samples N1 to N7 at 100°C.	57
5.9	Dielectric properties of samples N1 to N7 at 200°C.	58
5.10	Dielectric properties of samples N1 to N7 at 300°C.	59
5.11	Dielectric permittivity of sample (a) N3 and (b) N5 at 300°C.	61
5.12	Dielectric properties for the nickel zinc ferrites substituted with cobalt at room temperature with different composition.	62
5.13	Dielectric permittivity of sample CC plotted at various temperatures with the curve vertically shifted to avoid overlapping.	64
5.14	Arrhenius plot of the loss peak frequency, F_p of sample CC.	65
5.15	Dielectric properties of sample C1 at different temperature.	67
5.16	Dielectric properties for the nickel zinc ferrites substituted with cobalt at 100°C with different composition.	69
5.17	Dielectric properties for the nickel zinc ferrites substituted with cobalt at 200°C with different compositions.	70
5.18	Dielectric properties for the nickel zinc ferrites substituted with cobalt at 300°C with different compositions. Solid line has a gradient of -1 .	71
5.19	Dielectric properties of sample Y1 to Y5 at room temperature.	72
5.20	Loss factor for different samples with the curves vertically shifted up at room temperature.	74
5.21	A series of dielectric response of sample Y4 in the temperature range from 28°C to 300°C.	75



5.22	Activation Energy of samples YIG obtained from peak maximum at low frequency (LP) and high frequency (HP).	76
5.23	Effect of temperature on (a)dielectric permittivity (b)loss factor of sample Y5. The solid line has a gradient of -1 .	78
5.24	Dielectric permittivity versus frequency for sample Y1 to Y5 at 100°C	79
5.25	Dielectric permittivity versus frequency for sample Y1 to Y5 at 200°C	80
5.26	Dielectric permittivity versus frequency for sample Y1 to Y5 at 300°C	81
5.27	Dielectric response of sample CC at various temperatures.	83
5.28	Equivalent circuit representing the dielectric response for the sample CC from temperature 28°C to 150°C .	87
5.29	Equivalent circuit representing the dielectric response for the sample CC from temperature 200°C to 300°C .	87
5.30	Dielectric response of sample C2 at various temperatures.	91
5.31	Equivalent circuit representing the dielectric response in the sample C2 from temperature 28°C to 300°C .	94
5.32	Dielectric behaviour of sample N1 at various temperatures.	95
5.33	Dielectric behaviour of sample N2, N3, N6 and N7 at room temperature.	99
5.34	Dielectric response of sample N4 at various temperatures.	104
5.35	Equivalent circuit representing the dielectric response in the sample N4 from temperature 28°C to 150°C .	108
5.36	Equivalent circuit representing the dielectric response in the sample N4 from temperature 250°C to 300°C .	109
5.37	Dielectric response of sample N5 at various temperatures.	110
5.38	Equivalent circuit represented the dielectric response in the sample N5 from temperatures 28°C to 100°C	113
5.39	Dielectric response of sample Y1 at various temperatures.	114

5.40	Equivalent circuit represented the dielectric response in the sample Y1 from temperature 200°C to 300°C	118
5.41	Dielectric response of sample Y5 at various temperatures.	121
5.42	Equivalent circuit representing the dielectric response in the sample Y5 from temperature 28°C to 150°C	125
5.43	Equivalent circuit representing the dielectric response in the sample Y5 from temperatures 200°C to 300°C	125
5.44	Complex impedance plot of samples N1 to N4 at room temperature.	127
5.45	Complex impedance plot of samples N5 to N7 at room temperature.	128
5.46	Exploded view of impedance plot at high frequencies for sample N1 to N7 at room temperature.	128
5.47	Equivalent circuit used to represent the electrical properties in samples N1, N2, N4, N5, N6 and N7 at room temperature.	132
5.48	Equivalent circuit used to represent the electrical properties of in samples N3.	133
5.49	Complex impedance plots for sample N1 at different temperature.	136
5.50	Impedance Z'' spectroscopic plot for sample N1 at different temperatures.	140
5.51	Modulus M'' spectroscopic plot for N1 at different temperatures.	141
5.52	Impedance plot for different samples at room temperature.	144
5.53	Resistance of samples CC to C5 at room temperature obtained from impedance plot at low frequency end.	145
5.54	Exploded view of the different samples at room temperature at high frequency region.	146
5.55	Equivalent circuit used to represent the electrical properties in different samples at room temperature.	149



5.56	Complex impedance plot for the sample C1 at different temperatures.	151
5.57	Equivalent circuit used to represent the series resistance and grain boundary effects in sample C1 at temperature 100°C and above.	154
5.58	The invariant of the capacitance of the sample C1 at different temperatures.	155
5.59	Complex impedance plot of samples Y2 at various temperatures.	157
5.60	Equivalent circuit used to represent sample Y2 from 28°C to 100°C.	161
5.61	Equivalent circuit used to represent sample Y2 from 150°C to 300°C.	161
5.62	Complex impedance plots of sample Y5 at various temperatures.	163
5.63	Equivalent circuit used to represent sample Y5 at various temperature.	166
5.64	Ac conductivity of different samples at room temperature.	172
5.65	Ac conductivity of sample N1 at different temperatures.	174
5.66	Arrhenius plot of sample N1.	175
5.67	AC conductivity of different samples at room temperature.	176
5.68	Ac conductivity of sample CC at different temperatures.	177
5.69	Arrhenius plot of sample CC at 10 Hz.	178
5.70	AC conductivity of different samples at room temperature.	179
5.71	AC conductivity of sample Y1 at various temperatures.	180
5.72	Arrhenius plot of sample Y1 at 10 Hz.	181
5.73	DC resistivity of nickel zinc ferrites substituted with copper with different composition at room temperature.	182
5.74	Resistivity of samples (a) N1 to N4 and (b) N5 to N7 at different temperatures.	183



5.75	D.C Resistivity of nickel zinc ferrites substituted with copper with respect to reciprocal temperature.	184
5.76	Resistivity of samples CC to C5 at various temperatures.	186
5.77	Resistivity of samples CC to C5 at room temperature.	187
5.78	Arhenius plot of dc resistivity of sample CC to C5.	187
5.79	DC resistivity of YIG substituted with neodymium.	189
5.80	Arrhenius plot for sample Y1 to Y5.	190

